Identification of Parameters and Restoration of Motion Blurred Images

A Thesis Submitted
in Partial Fulfillment of the Requirements
for the Degree of
Master of Technology

by

Ravindra Yeshwant Lokhande

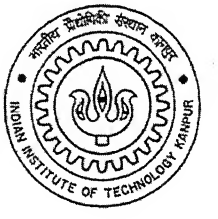

to the

Department of Computer Science & Engineering
Indian Institute of Technology Kanpur

December, 2004

Certificate

This is to certify that the work contained in the thesis entitled " *Identification of Parameters and Restoration of Motion Blurred Images* ", by *Ravindra Yeshwant Lokhande*, has been carried out under my supervision and that this work has not been submitted elsewhere for a degree.

December, 2004

P Gupta

(Prof. Phalguni Gupta)
Department of Computer Science & Engineering,
Indian Institute of Technology,
Kanpur.

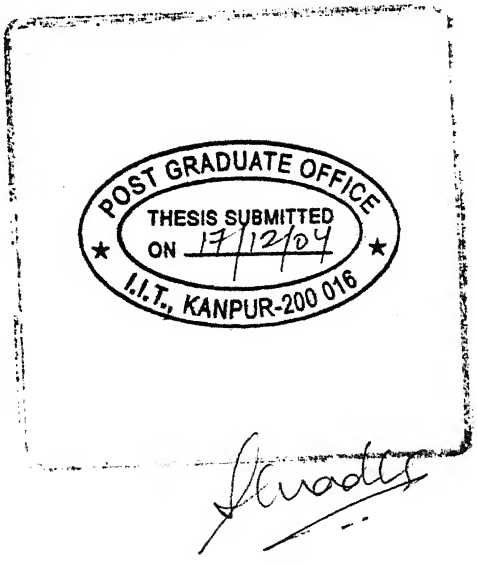

Abstract

The relative motion between the imaging system and an object, during the image formation process, results in a blurred image along the direction of the relative motion. For correct restoration of the blurred image, knowledge of the point spread function (PSF) is very important. The motion blur PSF is characterized by two parameters, namely blur direction and blur length. This thesis presents the methods that estimates the parameters of the PSF, from the blurred and noisy image itself. The estimation method, is based on the observation that image characteristics along the direction of motion are different than the characteristics in other directions. Blur direction is identified from the log spectrum of the blurred image, using the Hough transform. Blur length is identified by using the log spectrum of the blurred image which contains periodical minima relevant to the motion direction and length. The Wiener filter is used to restore the blurred and noisy image. The method is applied to artificial and real blurred images to determine the effectiveness of the method.

Acknowledgements

I would like to express my gratitude to all people, who supported me directly or indirectly for the completion of this work.

First of all, I would like to owe a debt of gratitude to my supervisor, Prof. Phalguni Gupta for his support and valuable guidance. I consider myself extremely fortunate to have had a chance to work under his supervision. In spite of his tight schedule he was always approachable and took his time off to attend to my problems.

I am highly obliged to all the faculty members of the Department of Computer Science and Engineering for the invaluable knowledge they have imparted to me. I also extend my thanks to the technical staff of the department for providing an excellent working facility.

I am thankful to all my batchmates, who make my stay at IIT Kanpur enjoyable and memorable. I would also like to thank Ashish Pandey, Aneesh Shukla, K.V. Arya and V.V. Saradhi for their help. My special thanks goes to Chandrakant Gaikwad for his support and encouragement.

Finally, I am grateful to my parents for taking me to this stage in life and teaching me the good things that really matters in life.

Contents

List of Tables

List of Figures

Chapter 1

Introduction

Images are captured to record or display useful information. Unfortunately, a recorded image invariably represents a degraded version of an original image or scene, due to imperfections in the imaging and capturing process. These degradations are classified into two categories: blur and noise. Images may be blurred due to defocussing of the lens, atmospheric turbulence, abberations in the optical systems, relative motion between the imaging system and the original scene.

In addition to these blurring effects, noise also degrades the image during the recording at the sensor. Noise may be introduced by the medium through which the image is created (random absorption or scatter effects), by the thermal motion of electrons in electronic components (electronic noise), by the statistical nature of light and the photoelectric conversion process in the image sensor (photoelectric noise), by the randomness of the silver halide grains in the film that records the image (film grain noise), by measurement errors due to the limited accuracy of the recording system, and by quantization of the data for digital storage.

The restoration of blurred and noisy image highly depends on the blurring system model used and on the accuracy by which its parameters are identified from the blurred and noisy image itself. The task of restoration can be divided into following two categories:

1. Blur identification - identify the parameters of the point spread function (PSF) from the observed degraded image itself.

2. Restoration - use of the identification procedure into the restoration algorithm.

1.1 Problem Definition

The successful restoration of blurred image requires accurate estimation of PSF parameters. In this thesis, we deal with images which are blurred by the relative motion between the imaging system and the original scene. Thus, given a motion blurred and noisy image, the task is to identify the point spread function parameters and apply the restoration filter to get an approximation to the original image.

In this thesis, we are identifying the parameters of the motion blur PSF and incorporating this knowledge into the restoration procedure. We use Wiener filter for the restoration. Parameter estimation is based on the observation that image characteristics along the direction of motion are different than the characteristics in other directions. The PSF of motion blur is characterized by two parameters namely, blur direction and blur length. For the detection of blur direction we use Hough transform to find the orientation of the line in the log magnitude spectrum of the blur image. Blur length is determined by rotating the log magnitude spectrum of the image in the estimated blur direction and then collapsing the 2-D data into 1-D vector and then performing inverse Fourier transform to yield the cepstrum, and finding the negative value in it.

1.2 Organization of the Thesis

In Chapter 2, the general model of degradation, the motion blur PSF and related work have been introduced. In Chapter 3, the basic of Fourier Transform and Hough transform is presented along with the methods for identifying the parameters of the motion blur PSF and the restoration filter. In Chapter 4, the experimental results are shown. Conclusion and future work have been given in Chapter 5.

Chapter 2

Background

The relative motion between an imaging system and an original scene during the image formation process results in a blurred image along the direction of the motion. The motion blurring effect can be reduced by increasing the shutter speed (which is relatively much faster than the motion of the object or camera). However, such a system with high shutter speed is expensive. So in order to remove the blurring effect from the image, we need to apply image processing techniques.

The field of *image restoration* (sometimes referred to as image deblurring or image deconvolution) is concerned with the reconstruction or estimation of the original undegraded image from the blurred and noisy one. Image restoration is distinct from image enhancement techniques. Image restoration techniques are oriented towards modeling the degradations, blur and noise whereas enhancement techniques are designed to manipulate an image in order to produce more pleasing results to an observer without making use of any particular degradation models [1, 12, 20]. Since exact restoration of the original scene from the observed image data may not be possible, even with knowledge of the degrading system characteristics, most filters developed try to improve the image to be as close as possible to the original scene.

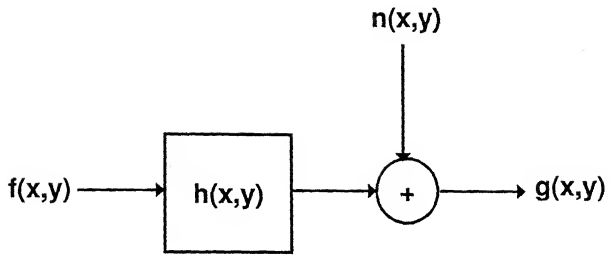

Figure 2.1: Image Degradation Model

2.1 Image Degradation Model

The degradation process is depicted in Figure 2.1, where the observed image $g(x, y)$ is modeled as the output of a 2-D linear system, which is characterized by its degradation function $h(x, y)$. The term $f(x, y)$ is an original image. The observation noise $n(x, y)$ is assumed to be a Gaussian distributed white noise with zero mean, which effectively models the noise in many different imaging scenarios.

When the degradation function $h(x, y)$ is linear and space-invariant system, then the observed image in spatial domain is mathematically expressed as,

$$\begin{aligned} g(x,y) &= h(x,y) * *f(x,y) + n(x,y) \\ &= \sum_{m=0}^{M-1} \sum_{n=0}^{N-1} h(x-m, y-n) f(x,y) + n(x,y) \end{aligned} \tag{1}$$

where $**$ indicates the two-dimensional convolution and g, h, f and n are observed image, degradation function, original image, and noise respectively, all of size M×N.

As convolution in the spatial domain is equal to multiplication in the frequency domain, equation (1) can be written in the frequency domain as,

$$G(u,v) = H(u,v)F(u,v) + N(u,v) \tag{2}$$

where (u,v) are the spatial frequency coordinates, and capital letters G, H, F and N are the Fourier transform of the observed image, degradation function, original image and noise respectively.

2.2 Motion Blur Function

In this thesis, we deal with images blurred by the uniform linear motion between the image and the sensor during image acquisition. When the scene to be recorded translates relative to the sensor at a constant velocity V_0 with an angle of θ degrees along the horizontal axis during the exposure interval $[0, T_e]$, the PSF $h(x, y)$ is given by equation (3), where "blur length" $L = V_0 * T_e$ [12, 18].

$$h(x,y) = \begin{cases} \frac{1}{L}, & 0 \leq |x| \leq L * \cos(\theta) \quad y = L * \sin(\theta) \\ 0, & otherwise \end{cases} \tag{3}$$

For the sake of simplicity and without loss of generality, let us assume that motion is along the horizontal direction i.e $\theta = 0°$, then equation (3) can be expressed as,

$$h(x,y) = \begin{cases} \frac{1}{L}, & 0 \leq |x| \leq L \quad y = 0 \\ 0, & otherwise \end{cases} \tag{4}$$

The Fourier transform of a 1-D function $f(x)$ is given by,

$$F(u) = \int_{-\infty}^{\infty} f(x) e^{-j2\pi ux} dx \tag{5}$$

So, taking Fourier transform of equation(4)

$$\begin{aligned} H(u) &= \int_0^L h(x) e^{-j2\pi ux} dx \\ &= \int_0^L \frac{1}{L} e^{-j2\pi ux} dx \\ &= \frac{1}{L} \int_0^L e^{-j2\pi ux} dx \\ &= \frac{1}{L} \left[\frac{e^{-j2\pi ux}}{-j2\pi u} \right]_0^L \\ &= \frac{-1}{j2\pi uL} \left[e^{-j2\pi uL} - 1 \right] \\ &= \frac{-1}{j2\pi uL} e^{-j\pi uL} \left[e^{-j\pi uL} - e^{j\pi uL} \right] \end{aligned}$$

Using $\sin x = \frac{1}{2j} [e^{jx} - e^{-jx}]$ in the above equation, we have:

$$H(u) = \frac{e^{-j\pi uL}}{j2\pi uL} \cdot j2 \sin(\pi uL)$$

$$
\begin{aligned}
&= \frac{\sin(\pi uL)}{\pi uL}.e^{-j\pi uL} \\
&= \operatorname{sinc}(\pi uL).e^{-j\pi uL}
\end{aligned} \tag{6}
$$

The magnitude transfer function of equation(6) is [8, 11, 13, 21],

$$
|H(u)| = \operatorname{sinc}(\pi uL) \tag{7}
$$

Note that H(u) is independent of the vertical frequency coordinate v. Similarly, the expression for motion blur PSF of blur length L whose direction is θ° with the horizontal axis can be obtained [2] and is given by,

$$
H(u,v) = \frac{\sin(\pi Lf)}{\pi Lf} \tag{8}
$$

where $f = u\cos\theta + v\sin\theta$.

2.3 Related Work

Restoration of motion blurred images requires the knowledge of its PSF, which is modeled as a mathematical equation as given by equation (3). This model in turn requires the knowledge of two parameters namely, blur direction and blur length. Many methods are available for finding these parameters.

From the Fourier magnitude of the blur PSF in equation (7) and its graphical representation in Figure 2.2, it is clear that $H(u,v) = \operatorname{sinc}(\pi Lu)$ is a periodic function with period $T = \frac{1}{L}$. Therefore after every $\frac{1}{L}$ there exist a zero crossing. The observed image is assumed to be the convolution of PSF $h(u,v)$ with the original image $f(u,v)$ and as convolution in spatial domain is equal to multiplication in frequency domain, the zero crossing also appears in the Power Spectrum of the blurred image. This zeros can be identified as a negative peak in the Cepstrum domain [2].

The technique of finding the negative peak is simple but if the blurred image is noisy they are obscured. In order to improve the peak detection [8], the blurred image is preprocessed to remove the noise by using *Spectral Subtraction* method [14]

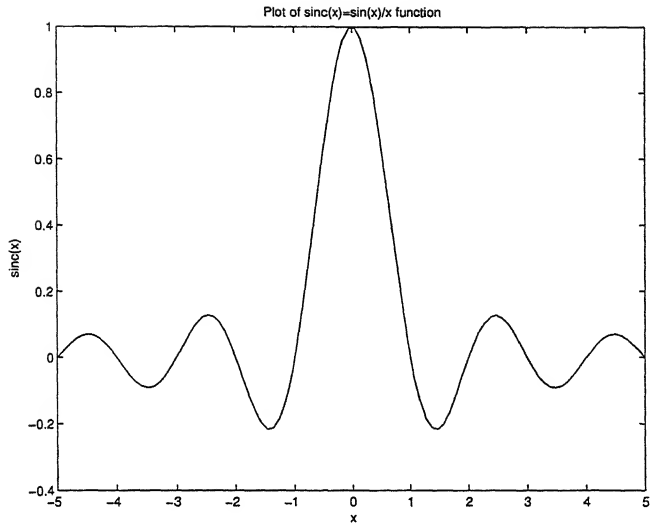

Figure 2.2: The Graphical representation of the sinc function.

and then transforming the enhanced spectral magnitude function in cepstral domain and the identification procedure is completed using an adaptive, quefrency-varying, "comb-like" window (lifter) [1]. The average of power spectrum is used for reducing noise, along the lines parallel to the expected minima and then examine the resulting one-dimensional spectral function to detect the minima in it [13]. The method used by [23] for identifying the blur length is based on the error characteristics due to the intentional use of inappropriate PSFs in the restoration process. The bispectrum of the blurred image is used to find the blur length in [3]. In [4] blur length is estimated, using the logarithmic regression and calculating the score in activity region. Gennery [9] tried to find the PSF parameter in the spectral domain.

Most of the work for parameter identification assumed that the motion is along the horizontal direction, which may not be the case in practical situation. [13] detects the blur direction by rotating the coordinate system for any specified direction θ varying from 0 to 180 degree and then computing its 1-D spectrum and inspect the

[1]The terms *quefrency* and *lifter* are commonly used in cepstral domain processing [5].

peaks and valleys in it. A direction θ is considered as the estimated motion direction if the peaks and valleys are more prominent in its 1-D spectrum than in those of all other directions. The use of steerable filter for the extraction of orientation is suggested in [18], where the second order derivative of a two dimensional Gaussian is used. The orientation is obtained by finding the highest response of the filter for any angle θ. An inertia-like tensor matrix approach is used in [15] where the central idea is to assess the anisotropy caused by motion blur in the degraded spectrum. In [6], blur direction is estimated in the Peak Trace Domain, which is based on the pole trace perpendicular to the direction of blur, made by main lobes of *sinc* function in the frequency domain.

Chapter 3

Identification of Parameters

In this chapter, the techniques for identifying the motion blur PSF parameters is presented. The first step towards successful restoration of blurred images, is the identification of blur parameters. After identifying the parameters the next step is to restore the blurred image using the restoration algorithm. We are using the Wiener filter [10] for the restoration of the blurred image. Figure 3.1 depicts the process of restoration of blurred image.

3.1 Fourier Transform

Both motion blur parameters namely, blur direction and blur length are calculated in the frequency domain and Fourier transform is the tool which transform the image from spatial domain to frequency domain and vice versa [10]. Therefore some working knowledge of Fourier transform is necessary. This section introduces Fourier transform and its properties.

3.1.1 Definition

Let f(x,y) be a continuous function of a real variables x and y. The Fourier transform (FT) of f(x,y), is defined by the equation

$$F(u,v) = \int_{-\infty}^{\infty} \int_{-\infty}^{\infty} f(x,y) e^{-j2\pi(ux+vy)}\, dx\, dy \qquad (1)$$

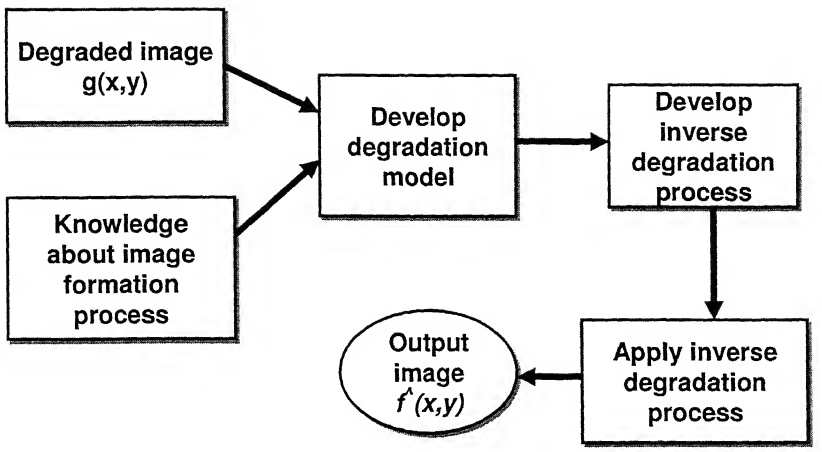

Figure 3.1: Image restoration process.

where $j = \sqrt{-1}$. Conversely, given $F(u, v)$, we can obtain $f(x, y)$ by using inverse Fourier transform (IFT)

$$f(x, y) = \int_{-\infty}^{\infty} \int_{-\infty}^{\infty} F(u, v) e^{j2\pi(ux+vy)} \, du \, dv \tag{2}$$

These two equations comprise the *Fourier transform pair.*

In image processing, the discrete version of above equations are used. The discrete Fourier transform (DFT) of a function (image) $f(x, y)$ of size $M \times N$ is given by the equation

$$F(u, v) = \Im\{f(x, y)\} = \frac{1}{MN} \sum_{x=0}^{M-1} \sum_{y=0}^{N-1} f(x, y) e^{-j2\pi(ux/M+vy/N)} \tag{3}$$

for values of $u = 0, 1, 2, ..., M - 1$, and also for $v = 0, 1, 2, ..., N - 1$. Similarly, given $F(u, v)$, we can obtain $f(x, y)$ using the inverse discrete Fourier transform (IDFT), given by the expression

$$f(x, y) = \Im^{-1}\{F(u, v)\} = \sum_{u=0}^{M-1} \sum_{v=0}^{N-1} F(u, v) e^{j2\pi(ux/M+vy/N)} \tag{4}$$

for values of $x = 0, 1, 2, ..., M - 1$, and also for $y = 0, 1, 2, ..., N - 1$. Equations (3) and (4) comprise the *two-dimensional, discrete Fourier transform (DFT) pair.*

The variables u and v are the *transform* or *frequency variables*, and x and y are the *spatial* or *image variables.*

Although an image $f(x, y)$ is a real function, we see from equation (3) that its Fourier transform $F(u, v)$ is, in general, a complex one. As in the analysis of complex numbers, it is convenient sometimes to express $F(u, v)$ in polar coordinates:

$$F(u, v) = |F(u, v)|e^{-j\phi(u,v)} \tag{5}$$

where

$$|F(u, v)| = \sqrt{R^2(u, v) + I^2(u, v)} \tag{6}$$

is called the *magnitude* or *spectrum* of the Fourier transform, and

$$\phi(u, v) = \tan^{-1}\left[\frac{I(u, v)}{R(u, v)}\right] \tag{7}$$

is called the *phase angle* or *phase spectrum* of the Fourier transform.

$$\begin{aligned} P(u, v) &= |F(u, v)|^2 \\ &= R^2(u, v) + I^2(u, v) \end{aligned} \tag{8}$$

is called *power spectrum* or *spectral density.* The terms $R(u, v)$ and $I(u, v)$ are the real and imaginary part of the $F(u, v)$ respectively.

In a number of applications the *power spectrum* is used, in order to identify different features. In lot of images although, *Fourier Spectra* decreases rapidly and the features are not recognizable, another function is used, in order to amplify the signal – the logarithm of the *Fourier Spectrum* plus one as shown in equation (9). This function has the property of keeping the zero values of the *Fourier Spectra* zero, and at the same time magnify small differences.

$$L(u, v) = \log(1 + |F(u, v)|) \tag{9}$$

3.1.2 Properties

One of the most common and important properties of Fourier transform is known as the *convolution theorem* which states that convolution in spatial domain is equal to multiplication in Fourier domain and also convolution in the Fourier domain reduces to multiplication in the spatial domain; that is,

$$f(x,y) * h(x,y) \iff F(u,v)H(u,v) \tag{10}$$

$$f(x,y)h(x,y) \iff F(u,v) * H(u,v) \tag{11}$$

Also, another basic property of Fourier transform that comes directly from its definition is linearity. Linearity enables us to break down a complicated function into simple ones as shown in the following equation.

$$\Im[\alpha f(x,y) + \beta h(x,y)] = \alpha\Im[f(x,y)] + \beta\Im[h(x,y)] = \alpha F(u,v) + \beta H(u,v) \tag{12}$$

If $f(x,y)$ is real, its Fourier transform is conjugate symmetric; that is,

$$F(u,v) = F^*(-u,-v) \tag{13}$$

where "*" indicates the standard conjugate operation on a complex number. From this, it follows that

$$|F(u,v)| = |F(-u,-v)|, \tag{14}$$

which says that the spectrum of the Fourier transform is symmetric.

The computational cost of the Fourier transform or its inverse in the discrete case is $O(n^2)$. Taking advantage of the separability property – which states that in the 2D FT we can perform first the summation over the first variable and then over the other independently – an algorithm has been developed which uses this property called Fast Fourier Transform (*FFT*) which calculates the DFT or IDFT in $O(n\log_2 n)$ time [10, 18]. We have used the FFT and IFFT for the computation of Fourier transform.

3.2 Cepstral Definition

The word *Cepstrum* is the anagram of the word *Spectrum* [5, 19]. Different definitions of the *Cepstrum* have been given, depending on the different applications. The most common definition of the *Cepstrum* of a function $g(x, y)$ is given by:

$$Cep\{g(x,y)\} = \Im^{-1}\{\log(G(u,v))\} \tag{15}$$

where $G(u, v)$ is the Fourier transform of a function $g(x, y)$. In other words, it is the *Inverse Fourier Transform* of the logarithm of the *Fourier Transform* of the signal. The *Cepstrum* is a complex function, but if we want only the real part then instead of the $G(u, v)$ we can take its magnitude as show below:

$$Cep\{g(x,y)\} = \Im^{-1}\{\log(1+|G(u,v)|)\} \tag{16}$$

3.3 Hough Transform

The Hough Transformation (HT) was invented in 1962 by P.V.C.Hough, and plays an important role in computerized image processing [10, 17, 22]. In theory, it can detect any arbitrary shapes in images, given a parameterized description of the shape in question. In practice, however it is generally used for finding only straight lines or circles as the computational complexity of the method grows rapidly with more complex shapes . Here we are using HT for line detection.

The general equation of a straight line in slope-intercept form is given by,

$$y = mx + c \tag{17}$$

where m is the slope and c is the y-intercept of the line. Let (x_1, y_1) be any point in the xy-plane, there could be an infinite number of lines that can pass through this point, but they all satisfy the equation $y_1 = mx_1 + c$ for varying values of m and c. However, writing this equation in the *parameter space* (m, c) as $c = -mx_1 + y_1$, yields the equation of a single line for a fixed point (x_1, y_1). Furthermore, a second point (x_2, y_2) also has a line in parameter space associated with it, and this line intersects

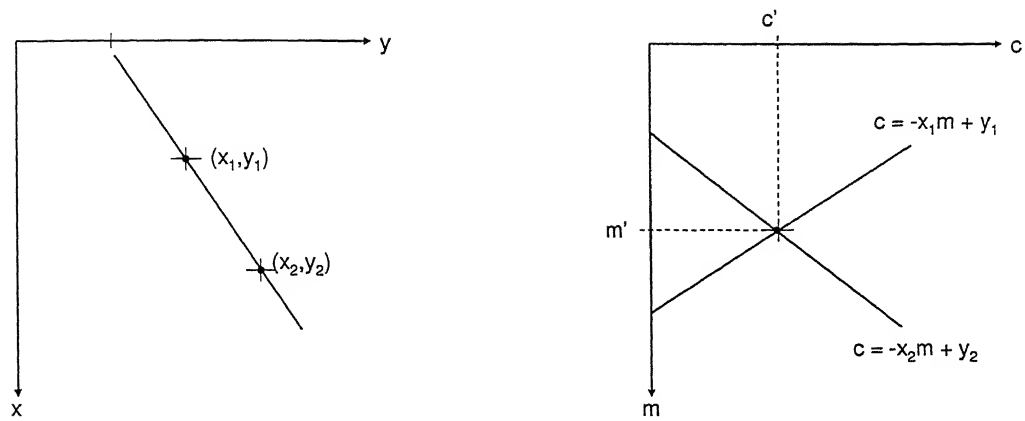

(a) (b)

Figure 3.2: (a) Straight line on the image plane (b) its representation in the parameter space

the line associated with (x_1, y_1) at (m', c'). The intersection (m', c') of these two lines determines uniquely the straight line passing through $(x_i, y_i), i = 1, 2$. In fact, all points contained on this line have lines in parameter space that intersect at (m', c') (Figure 3.2).

The problem with parametric model (equation (17)) is that the slope approaches infinity as the line approaches the vertical. The solution to this problem was suggested in [7] which uses the normal representation of a straight line given by:

$$\mathrm{r} = \mathrm{x}\cos\theta + \mathrm{y}\sin\theta \tag{18}$$

where r is the length of a normal from the origin to this line and θ is the orientation of r with respect to the X-axis as show in Figure 3.3. In this representation θ is bounded by $[0, 2\pi]$ and r is bounded by size of the image. A line passing through the point (x_1, y_1) represents a sinusoidal curve $\mathrm{r} = x_1\cos\theta + y_1\sin\theta$ in the parameter space (r, θ). Collinear points (x_i, y_i) on the image space correspond to intersections of sinusoids on the parameter space.

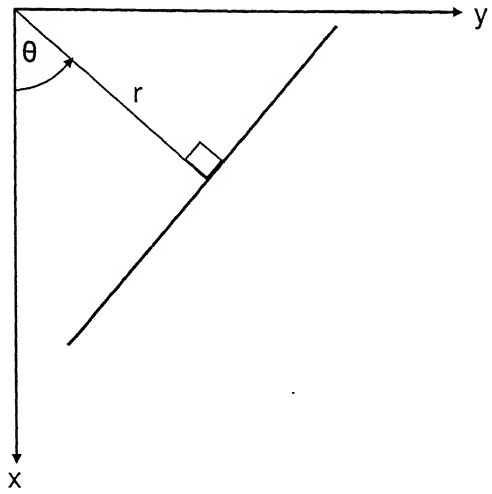

Figure 3.3: Normal representation of a line

The Hough transform divides the parameter space into so-called *accumulator cells*. For each point (x_i, y_i) in the image, the corresponding curve given by equation (18) is entered in the accumulator by incrementing the count in each cell along the curve. Thus, a given cell in the two-dimensional accumulator eventually records the total number of curves passing through it. After all image points have been treated, the accumulator is inspected to find cells having high counts. If the count in a given cell (r_i, θ_j) is N, then N image points lie along the line whose normal parameters are (r_i, θ_j). The detailed algorithm for finding line in a image is given below:

1. Let θ_{min} and θ_{max} be the minimum and maximum values of θ.

2. Initialize the accumulator array $\mathtt{A(r,}\theta\mathtt{)}$ to zero.

3. For each image point (x_i, y_i)

   For θ = θ_{min} to θ_{max}

   {

   $\mathrm{r} = x_i \cos\theta + y_i \sin\theta$

   $\mathtt{A(r,}\theta\mathtt{)}$ = $\mathtt{A(r,}\theta\mathtt{)}$ + 1

   }

4. Find the maximum value in the accumulator array A. The position in the array A(r_m, θ_m) where this maximum value occurs corresponds to the r and θ values that represent the line $r_m = x\cos\theta_m + y\sin\theta_m$.

3.4 Blur Direction Identification

The identification of blur direction is based on the observation that the spectrum of unblurred image is isotropic, whereas the spectrum of motion blurred image is anisotropic (Figure 3.4).

An image blurred due to motion is usually represented by a linear system of a convolution $g(x,y) = f(x,y) * *h(x,y)$, with h(x,y) the convolution kernel that causes the motion blur. The motion blur kernel low-passes the image in the direction of the blur. If we take the spectrum of the blurred image, then we can see that the most of the energy is in the direction, perpendicular to the motion direction. This can be seen as a line in binary spectrum as shown in Figure 3.5(a). So in order to determine the blur direction, we are treating the spectrum as an image. Then Hough transform (Section 3.3) is used to detect the orientation of the line in the spectrum. To reduce the computation cost of the Hough transform we binarized the spectrum. Also it is observed that most of the energy is concentrated in the central part of the spectrum, so we can reduce the computation cost by using only the central part of the spectrum. The Hough transform returns the accumulator array in which we locate the highest value which corresponds to the blur direction as shown in Figure 3.5(b). The Hough transform detects the line even in the presence of noise. The detailed algorithm for blur direction identification is as follows:

1. Let g(x,y) be the blurred image and G(u,v) be its Fourier transform.
2. Calculate the Fourier transform G(u,v) of the blurred image g(x,y).
3. Calculate the log spectrum of G(u,v) and convert it to binary.
4. Call Hough transform which returns the accumulator array.

5. Find the maximum value in the accumulator array which corresponds to blur direction.

3.5 Blur Length Identification

After the blur direction estimation, next task is to find the *blur length.* The identification of blur length requires the knowledge of blur direction.

As discussed in Chapter 2, the Fourier transform of observed image is the multiplication of Fourier transform of PSF and original image, if noise is neglected. The frequency response of the PSF is given by equation (6). The magnitude of the blur function is given by equation (7), which is characterized by periodic zeros on the u axis which occurs at

$$u = \pm\frac{1}{L}, \pm\frac{2}{L}, \pm\frac{3}{L}, \ldots \tag{19}$$

That is zero crossings would occur periodically in $H(u, v)$ or equivalently in $G(u, v)$ along lines perpendicular to the motion direction. So by looking for zero in $G(u, v)$ we can determine the blur length, but $G(u, v)$ is complex so instead of finding the zeros in it, we would detect minima in real spectrum. If we transform this spectrum in cepstral domain we can observe the negative peak.

For estimation of blur length, the spectrum is converted to binary and then rotated in the opposite direction (which is identified in Section 3.4). After this the 2-D data is converted to 1-D by averaging it along the columns. Then inverse Fourier transform is performed and the first negative value is searched, which corresponds to the blur length (Figure 3.6). Rather than taking the negative peak, we are taking the first negative value which we found to be more appropriate as compared to negative peak. The detailed algorithm for identifying the blur length is as follows:

1. Let g(x,y) be the blurred image and G(u,v) be its Fourier transform.
2. Calculate the Fourier transform G(u,v) of the blurred image g(x,y).
3. Calculate the log spectrum of G(u,v) and convert it to binary.

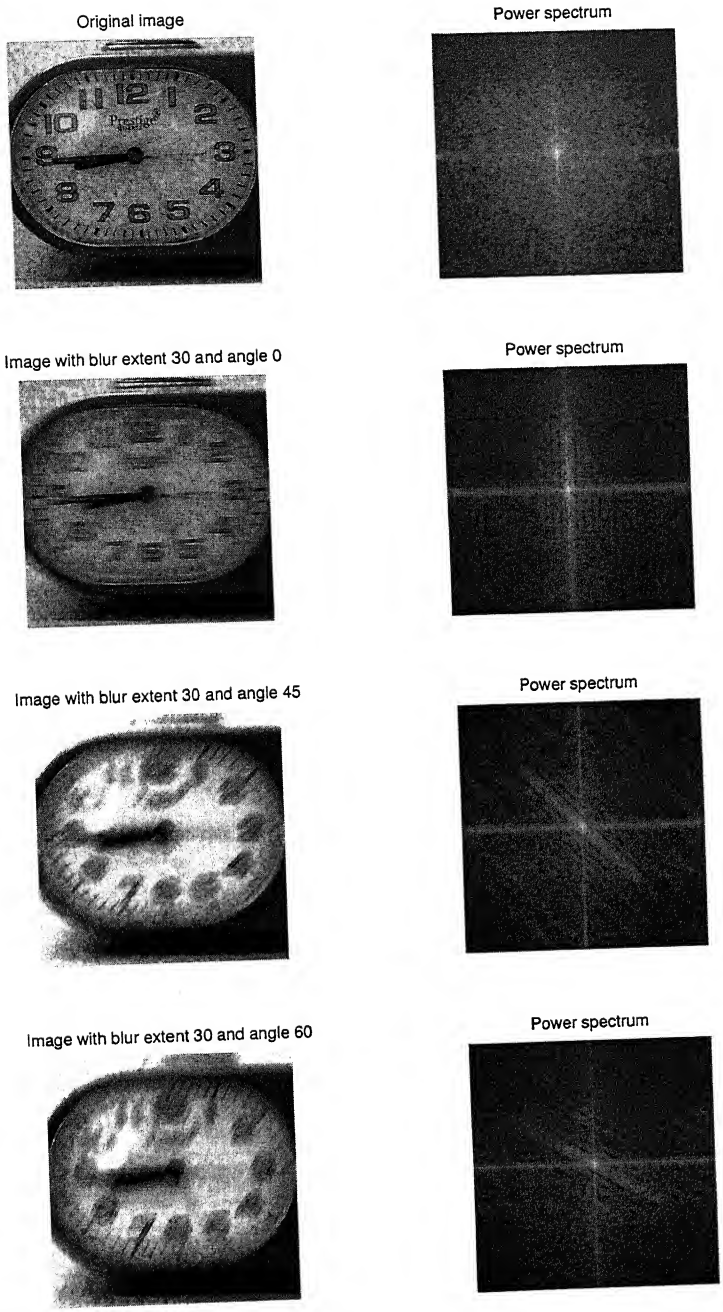

Figure 3.4: Figure showing image and their spectrum

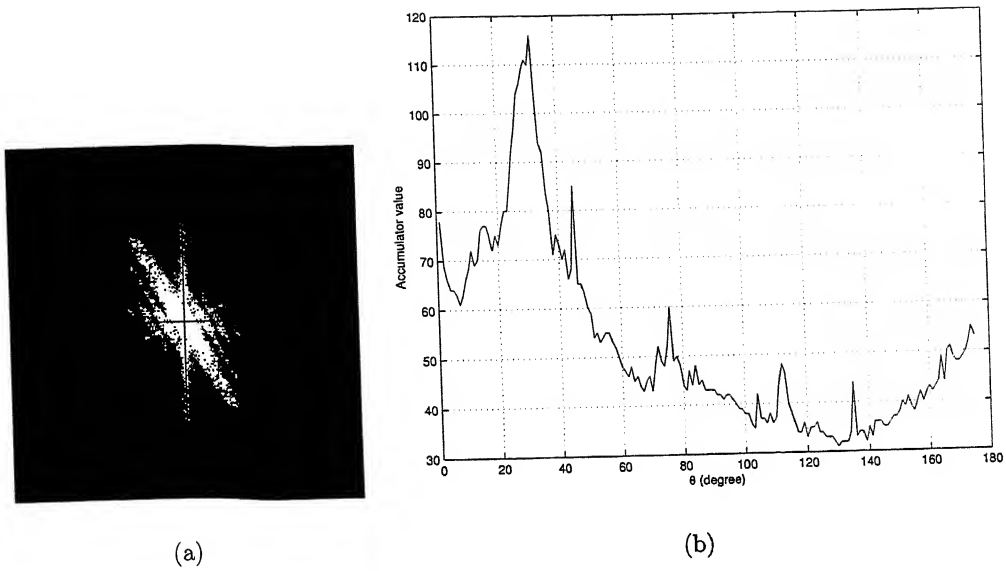

(a) (b)

Figure 3.5: (a) Spectrum of the blurred image with blur length 30 and direction 30 degree (b) Figure showing maximum value at 30 degree

4. Rotate the binary spectrum in the opposite direction(which is obtained from the previous algorithm).

5. Collapse the 2-D data into 1-D by taking the average along the columns.

6. Take the inverse Fourier transform of the output obtained from the previous step and locate the first negative value in the real part, which corresponds to the blur length.

In case of noise, the same procedure is followed with the exception that the blurred image is *averaged filtered* before taking its spectrum. We assume white Gaussian noise with zero mean which effectively model the noise in many different imaging scenarios and average filter effectively removes the Gaussian noise [10, 16, 22].

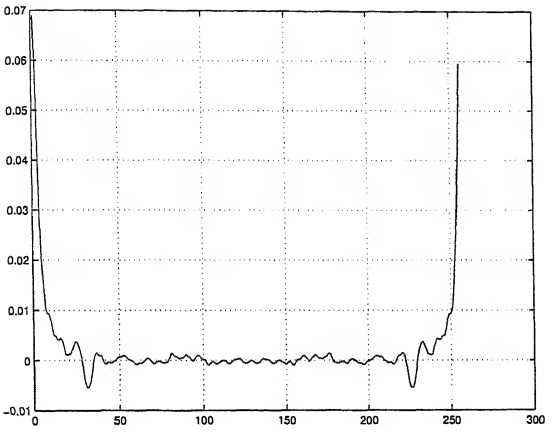

Figure 3.6: Figure showing the first negative value at 29

3.6 Image Restoration

Blurred image restoration is carried out as the next step after the identification of PSF parameters. The exact restoration of the original scene from the blurred image may not be possible, even with knowledge of the degrading system characteristics, most filters developed try to improve the image to be as close as possible to the original scene. There are several methods that can be used for the restoration of blurred image. These methods are divided into two categories [24]: the direct methods and the indirect methods. In direct methods the image restoration is carried out in one step whereas the indirect methods use iterative techniques.

3.6.1 Inverse Filter

The simplest method to restore the image is inverse filtering, where an estimate of the original image $\hat{F}(u,v)$ is obtained by dividing the Fourier transform of the degraded image $G(u,v)$ by the degradation function $H(u,v)$ as given by:

$$\hat{F}(u,v) = \frac{G(u,v)}{H(u,v)} = G(u,v)\frac{1}{H(u,v)} \tag{20}$$

The problem with above equation is that $\frac{1}{H(u,v)}$ does not necessarily exist. If $H(u,v) = 0$ or is close to zero, it may not be computationally possible to compute $\frac{1}{H(u,v)}$. Another problem with inverse filtering is that it does not perform well for noisy images. Using $G(u,v) = F(u,v)H(u,v) + N(u,v)$ in equation (20), we get

$$\begin{aligned} \hat{F}(u,v) &= \frac{F(u,v)H(u,v) + N(u,v)}{H(u,v)} \\ \hat{F}(u,v) &= F(u,v) + \frac{N(u,v)}{H(u,v)} \end{aligned} \tag{21}$$

As we can see from the above equation that when $H(u,v)$ has zero or very small value (which is often the case with motion blur), the ratio $N(u,v)/H(u,v)$ dominates the estimate $\hat{F}(u,v)$, which results in poor restoration.

3.6.2 Wiener Filter

As discussed in the previous section, inverse filter performs poorly in the presence of noise, we are using Wiener filter for the restoration of blurred image.

Wiener filter [10] considers images and noise as random process, and aims to find an estimate $\hat{f}$ of the ideal image f such that the mean square error between them is minimized. This error measure is given by

$$e^2 = E[(f - \hat{f})^2] \tag{22}$$

where $E[\cdot]$ is the expected value of the argument. It is assumed that the noise are uncorrelated, that is one or the other has zero mean. Based on these conditions, the minimum of the error function in equation (22) is given in the frequency domain by the expression

$$\begin{aligned} \hat{F}(u,v) &= \left[\frac{H^*(u,v)S_f(u,v)}{S_f(u,v)|H(u,v)|^2 + S_n(u,v)}\right] G(u,v) \\ &= \left[\frac{H^*(u,v)}{|H(u,v)|^2 + S_n(u,v)/S_f(u,v)}\right] G(u,v) \end{aligned} \tag{23}$$

where

$H(u,v)$ = frequency response of PSF $h(x,y)$

$$
\begin{aligned}
H^*(u,v) &= \text{complex conjugate of } H(u,v) \\
|H(u,v)|^2 &= H^*(u,v)H(u,v) \\
S_n(u,v) &= |N(u,v)|^2 = \text{power spectrum of the noise} \\
S_f(u,v) &= |F(u,v)|^2 = \text{power spectrum of the original undegraded image.}
\end{aligned}
$$

This filter is also referred as *minimum mean square error filter* or the *least square error filter*. The restored image in the spatial domain is given by the inverse Fourier transform of the frequency domain estimate $\hat{F}(u,v)$ i.e $\hat{f} = \Im^{-1}\{\hat{F}(u,v)\}$. If the noise is zero, then the noise power spectrum vanishes and the Wiener filter reduces to the inverse filter.

When the noise is white, then its spectrum $|N(u,v)|^2$ is a constant. Equation (23), requires the knowledge of power spectrum of original undegraded image, which we seldom know. Therefore equation (23) can be approximated to the following expression

$$\hat{F}(u,v) = \left[\frac{H^*(u,v)}{|H(u,v)|^2 + K}\right] G(u,v) \tag{24}$$

where K is a constant. One can determine the value of K through experiments. We have found through experiments that the good approximation for the value of K is, $K = 1/iw$, where iw is the width of the image.

The detailed algorithm for the restoration of motion blurred image is as follows:

1. Identify the blur direction using the method described in Section 3.4.

2. Identify the blur length using the method described in Section 3.5.

3. Form the PSF by using the blur direction and blur length and calculate its Fourier transform $H(u,v)$.

4. Calculate the Wiener filter which is given by,

$$W(u,v) = \left[\frac{H^*(u,v)}{|H(u,v)|^2 + K}\right] \tag{25}$$

5. Obtained $\hat{F}(u,v)$ by multiplying the Fourier transform of blurred image $G(u,v)$ with $W(u,v)$ i.e. $\hat{F}(u,v) = W(u,v)G(u,v)$

6. Obtained the restored image by taking the inverse Fourier transform of $\hat{F}(u,v)$ i.e. $f(x,y) = \Im^{-1}\{\hat{F}(u,v)\}$

Figure 3.7 shows blurred image of Book cover with blur direction 0 degree and blur length 15. Figure 3.8(a) shows the restored image obtained by using the inverse filter and Figure 3.8(b) shows the result obtained using the Wiener filter. We can see the difference between the restored image obtained by using inverse filter and by using Wiener filter. Wiener filter produces good restored image whereas the result obtained by inverse filter is useless.

Figure 3.7: Book cover blurred image with blur length 15 and direction 0 degree

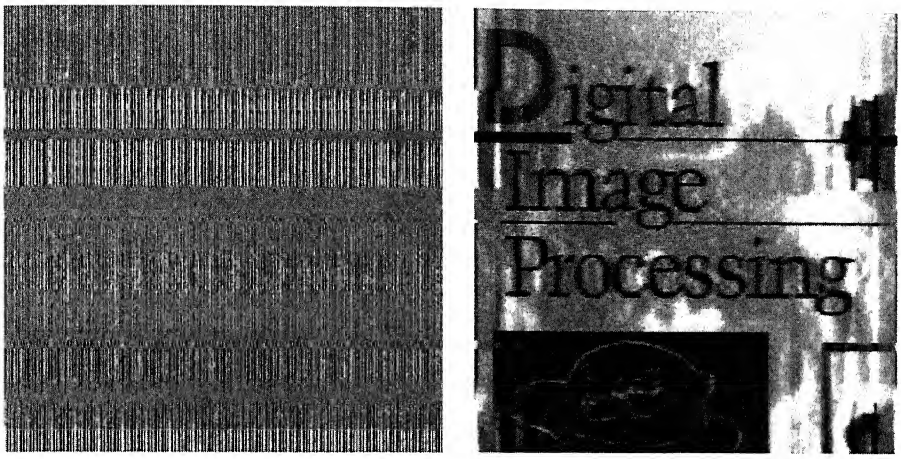

(a) Restored image obtained by using inverse filter

(b) Restored image obtained by using Wiener filter

Figure 3.8: Restoration result

Chapter 4

Experimental Results

In this chapter, we presents the results obtained by using the methods described in Chapter 3. The experiments are performed on artificially blurred images and real blurred images. We have used gray scale images with 256 gray levels. The images which are blurred artificially for experiments are shown in Figure 4.1.

The images shown in Figure 4.1 are artificially blurred with different blur lengths and directions. The 2nd and 3rd columns of Table 4.1, shows the blur length and direction used for blurring the images without adding any noise whereas last column shows the blur direction identified by using the method described in Section 3.4. Similarly the 2nd and 3rd columns of Table 4.2 shows the blur length and blur direction used for blurring the images whereas last column indicates the blur length identified by the method described in Section 3.5.

Table 4.3 and Table 4.4, shows the detected blur direction and blur length for blurred and noisy images. The 2nd, 3rd and 4th columns of Table 4.3 shows the blur length, direction and amount of added noise respectively whereas the last column indicates the detected blur direction. Similarly, the 2nd, 3rd and 4th columns of Table 4.4 show the blur length, direction and amount of added noise respectively whereas the last column shows the detected blur length.

Figure 4.2(a) shows the artificially blurred image with blur direction 45 degree and length 45 and Figure 4.2(b) shows the corresponding restored image. Figure

(a) Cameraman 256 x 256

(b) Lena 256 x 256

(c) Book Cover 325 x 324

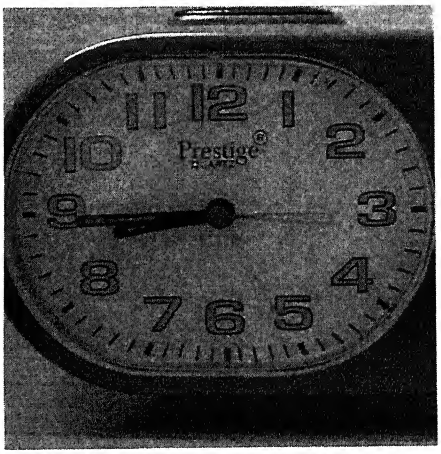

(d) Watch 478 x 478

Figure 4.1: Images used for experiments

Images	Blur Length	Blur Direction (Degree)	Detected Blur Direction
Cameraman	10	0	0
	15	50	45
	25	13	11
	30	55	55
	75	0	0
Lena	13	0	0
	20	60	58
	27	0	0
	30	70	70
	42	30	29
Book cover	15	0	0
	15	30	29
	23	18	18
	38	30	31
	60	40	39
Watch	15	45	45
	20	50	45
	30	45	45
	35	15	14
	50	0	0

Table 4.1: Table showing detected blur direction of blurred images

Images	Blur Length	Blur Direction (Degree)	Detected Blur Length
Cameraman	10	0	10
	15	50	15
	25	13	25
	30	55	29
	75	0	72
Lena	13	0	14
	20	60	18
	27	0	28
	30	70	26
	42	30	33
Book cover	15	0	16
	15	30	15
	23	18	22
	38	30	35
	60	40	53
Watch	15	45	15
	20	50	13
	30	45	28
	35	15	31
	50	0	44

Table 4.2: Table showing detected blur length of blurred images

Images	Blur Length	Blur Direction (Degree)	Noise Variance	Detected Blur Direction
Cameraman	20	15	130.05	16
	20	45	325.125	45
	25	15	130.05	14
	30	20	65.025	21
	50	10	65.025	11
Lena	13	40	65.025	45
	20	42	130.05	45
	22	45	65.025	45
	35	25	130.05	25
	42	20	65.025	22
Book cover	15	20	65.025	22
	15	45	195.075	45
	23	18	195.075	19
	35	0	130.05	0
	38	30	130.05	31
Watch	20	42	130.05	45
	32	47	65.025	45
	35	45	65.025	45
	37	15	130.05	15
	40	10	130.05	10

Table 4.3: Table showing detected blur direction of blurred and noisy images

Images	Blur Length	Blur Direction (Degree)	Noise Variance	Detected Blur Length
Cameraman	20	15	130.05	20
	20	45	325.125	18
	25	15	130.05	22
	30	20	65.025	30
	50	10	65.025	49
Lena	13	40	65.025	14
	20	42	130.05	18
	22	45	65.025	20
	35	25	130.05	30
	42	20	65.025	44
Book cover	15	20	65.025	16
	15	45	195.075	9
	23	18	195.075	22
	35	0	130.05	34
	38	30	130.05	29
Watch	20	42	130.05	20
	32	47	65.025	31
	35	45	65.025	34
	37	15	130.05	33
	40	10	130.05	34

Table 4.4: Table showing detected blur length of blurred and noisy images

4.2(c) shows the blurred Lena image with blur direction 30 degree and length 20 and Figure 4.2(d) shows the corresponding restored image. Figure 4.3(a) shows the blurred book cover image with blur direction 30 degree and length 38 and Figure 4.3(b) shows the corresponding restored image. Figure 4.3(c) shows the watch image blurred with blur direction 60 degree and length 30 and Figure 4.3(d) shows the corresponding restored image.

The Figure 4.4 shows the restoration result of blurred and noisy images. The Figure 4.4(a) is the book cover image blurred with direction 18 degree and length 23 with additive white Gaussian noise of variance 325 and Figure 4.4(b) shows the corresponding restored image. The Figure 4.4(c) is the watch image blurred with direction 42 and length 20 with additive white Gaussian noise of variance 130 and the corresponding restored image is shown in Figure 4.4(d).

Figure 4.5(a) shows the calender image taken by digital camera. The image is blurred due to camera motion. The detected blur direction is 0 degree and blur length is 47. Figure 4.5(b) shows the restored image. Similarly Figure 4.6(a) shows the image of a bus number plate. Figure 4.6(b) shows the restored image. The detected blur direction is 15 degree and blur length is 28.

(a) Blurred Cameraman image with blur length 25 and direction 45 degree

(b) Restored image

(c) Blurred Lena image with blur length 20 and direction 30 degree

(d) Restored image

Figure 4.2: Restoration result

(a) Blurred Book cover image with blur length 38 and direction 30 degree

(b) Restored image

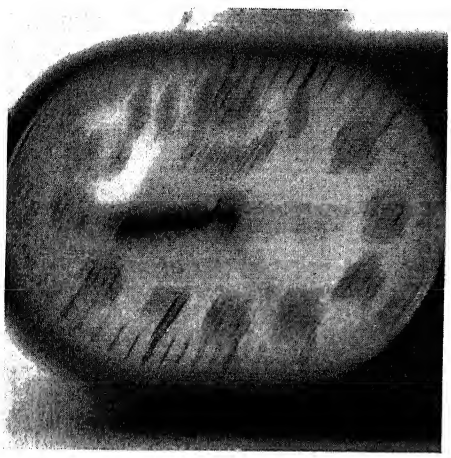

(c) Blurred Watch image with blur length 30 and direction 60 degree

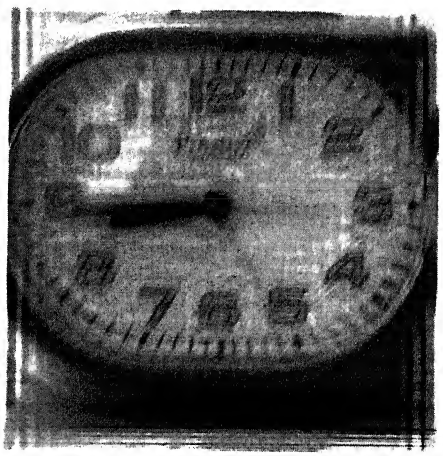

(d) Restored image

Figure 4.3: Restoration result

(a) Blurred and noisy Book cover image with blur length 23, direction 18 degree and variance 325

(b) Restored image

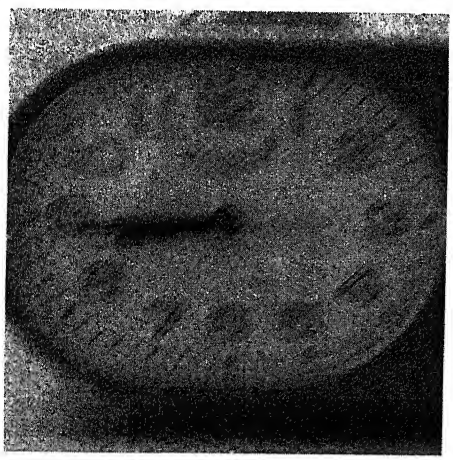

(c) Blurred and noisy Watch image with blur length 20,direction 42 degree and variance 130

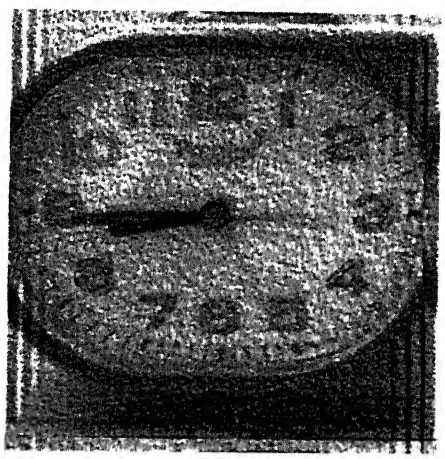

(d) Restored image

Figure 4.4: Restoration result

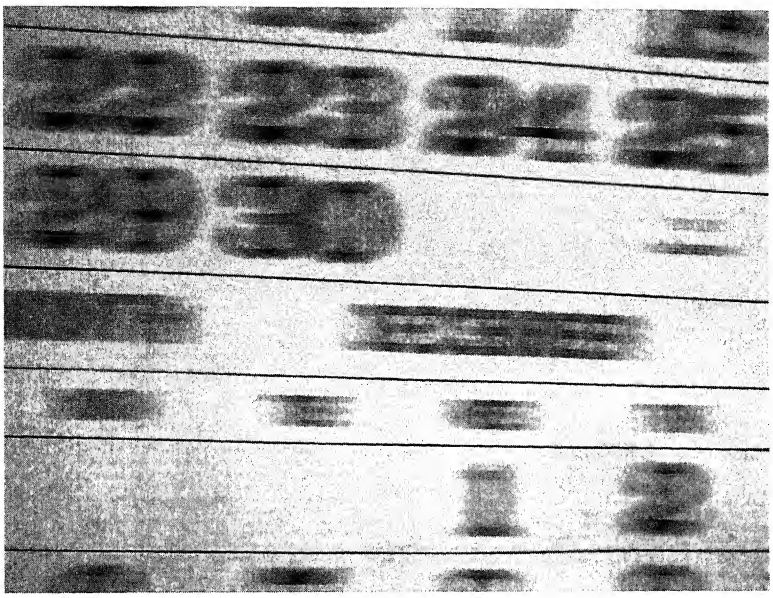

(a) Calender image, size 480 x 640

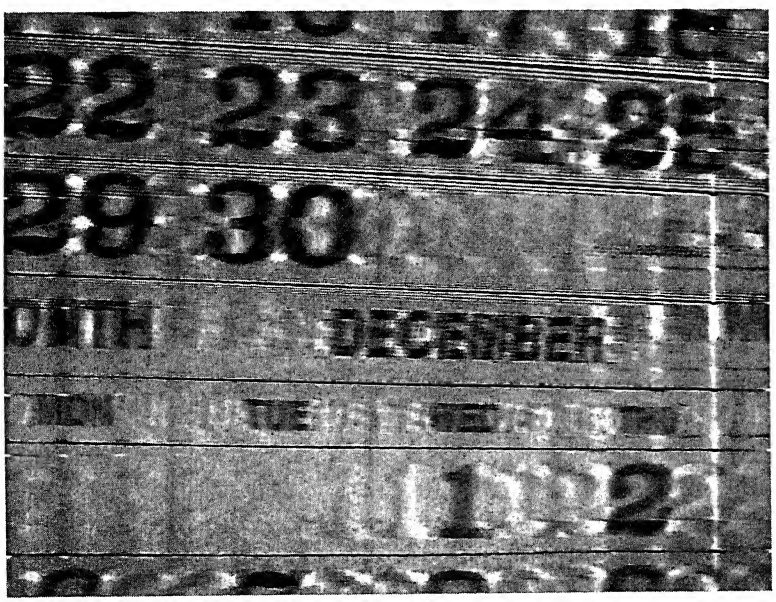

(b) Restored image

Figure 4.5: Restoration result

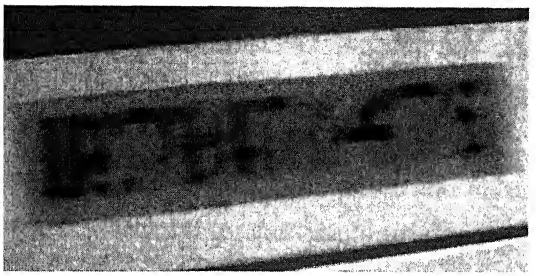

(a) Bus number plate image, size 230 x 466

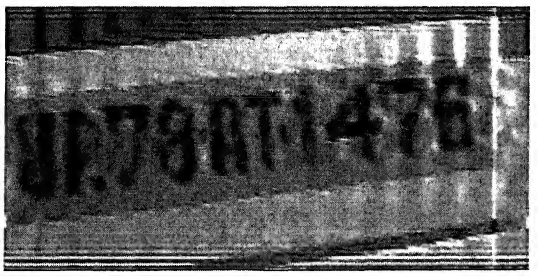

(b) Restored image

Figure 4.6: Restoration result

Chapter 5

Conclusion and Future Work

Due to the relative motion between an imaging system and an original scene during the image formation process, observed images are blurred along the direction of the relative motion. The motion blur PSF is characterized by two parameters namely, blur direction and blur length. Most of the methods consider the motion, along the horizontal direction which may not be the case in real life.

In this thesis, we have proposed the methods for the identification of motion blur PSF parameters. The proposed methods are based on the observation that image characteristics along the direction of motion are different than the characteristics in other directions. The algorithm operates in the frequency domain.

The blur direction is estimated using the Hough transform, which finds the direction in the spectrum of the blurred image and this information is used to determine the blur length. The blur length is obtained by rotating the binarized spectrum in the estimated direction and then collapsing the 2-D data to 1-D and taking the inverse Fourier transform and finding the first negative value. After identifying the PSF parameters the blurred image is restored by using the parametric Wiener filter.

There is always scope for future development in any work. Here we suggests some future development that could follow. The computation time of algorithm can be minimized by parallel implementation. We have deal with gray scale images so it

can be extended to work on true color images. The blur direction method is quite robust as compared to blur length method, because in the presence of noise the former method's output slightly varies from the actual direction whereas the later method's output sometimes vary significantly from the correct length. So one can try to improve the robustness of blur length algorithm.

The algorithm can be used in various applications, such as medical imaging, computer vision, forensic science field etc.. So depending upon the application, it may require some changes. Also application specific issues should be addressed such as speed versus accuracy, acceptable error levels and others.

Bibliography

[1] M. R. Banham and A. K. Katsaggelos. Digital Image Restoration. *IEEE Signal Processing Magazine*, 14(2):24–41, 1997.

[2] M. Cannon. Blind Deconvolution of Spatially Invariant Image Blurs with Phase. *IEEE Trans. Acousatic Speech and Signal Processing*, 24(1):56–63, 1976.

[3] M. M. Chang, A. M. Tekalp, and A. T. Erdem. Blur Identification Using the Bispectrum. *IEEE Trans. on Signal Processing*, 39(10):2323–2325, 1991.

[4] Yung-Sheng CHEN and I-San CHOA. An Approach to Estimating the Motion Parameters for a Linear Motion Blurred Image. *IEICE Trans. Inf. and Syst.*, E83-D(7):1601–1603, 2000.

[5] D. G. Childers. The Cepstrum: A Guide to Processing. *Proc. IEEE*, 65(10):1428–1443, 1997.

[6] Ji Woong Choi, Moon Gi Kang, and Kyu Tae Park. An Algorithm to Extract Camera-shaking Degree and Noise Variance in the Peak-trace Domain. *IEEE Transactions on Consumer Electronics*, 44(3):1159–1168, 1998.

[7] R. O. Duda and P. E. Hart. Use of the Hough Transformation to Detect Lines and Curves in Pictures. *Communications of the ACM*, 15(1):11–15, 1972.

[8] R. Fabian and D. Malah. Robust Identification of Motion and Out-of-focus Blur Parameters from Blurred and Noisy Images. *CVGIP: Graphical, Models and Image Processing*, 53:403–412, 1991.

[9] D. B. Gennery. Determination of Optical Transfer Functioin by Inspection of Frequency Domain Plot. *JOSA*, 63(12):1571–1577, 1973.

[10] R. C. Gonzalez and R. E. Woods. *Digital Image Processing.* Pearson Education, 2003.

[11] O. Hadar, I. Dror, and N.S. Kopeika. Image resolution limits resulting from mechanical vibrations. Part IV: real-time numerical calculation of optical transfer functions and experimental verification. *Optical Eng.*, 33(2):566–578, 1994.

[12] R. L. Lagendijk and J. Biemond. Basic Methods for Image Restoration and Identification.

[13] Qiang Li and Yasuo Yoshida. Parameter Estimation and Restoration for Motion Blurred Images. *IEICE Trans. Fundamentals*, E80-A(8), 1997.

[14] J. S. Lim. Image Restoration by Short Space Spectral Substraction. *IEEE Trans. Acoust Speech Signal Process.*, 28(2):191–197, 1980.

[15] Claudia Mayntz, Til Aach, and Dietmar Kunz. Blur Identification Using a Spectral Inertia Tensor and Spectral Zeros. In *ICIP (2)*, pages 885–889, 1999.

[16] H. R. Myler and A. R. Weeks. *Computer Imaging Recipes in C.* Prentice Hall, 1993.

[17] I. Pitas. *Digital Image Processing Algorithms And Applications.* John wiley and Sons, Inc., 2000.

[18] Ioannis Rekleitis. Visual Motion Estimation based on Motion Blur Interpretation. Master's thesis, School of Computer Science, McGill University, 1995.

[19] R. Rom. On the Cepstrum of Two-Dimensional Functions. *IEEE TRANS. Inf. Theory*, IT-21:214–217, 1975.

[20] M. I. Sezan and A. M. Tekalp. Survey of Recent Developments in Digital Image Restoration. *Optical Engg.*, 29(5):393–404, 1990.

[21] S. C. Som. Analysis of the Effect of the Linear Smear on Photographic Images. *JOSA*, 61(7):859–864, 1971.

[22] Scott E. Umbaugh. *Computer Vision and Image Processing: A Practical Approach Using CVIPtools.* Prentice Hall, 1998.

[23] Y. Yitzhaky and N. S. Kopeika. Identification of Motion Blur for Blind Image Restoration. In *IEEE symposium on Electro-optics*, 1995.

[24] Yitzhak Yitzhaky, Ruslan Milberg, Sergei Yohaev, and Norman S. Kopeika. Comparision of Direct Blind Deconvolution Methods for Motion-blurred Images. *Applied Optics*, 38(20):4325–4332, 1999.